



CHORUS

This is the accepted manuscript made available via CHORUS. The article has been published as:

Magnetic form factor of the deuteron in chiral effective field theory

S. Kölling, E. Epelbaum, and D. R. Phillips

Phys. Rev. C **86**, 047001 — Published 10 October 2012

DOI: [10.1103/PhysRevC.86.047001](https://doi.org/10.1103/PhysRevC.86.047001)

The magnetic form factor of the deuteron in chiral effective field theory

S. Kölling,^{1,*} E. Epelbaum,^{1,†} and D. R. Phillips^{2,‡}

¹*Institut für Theoretische Physik II, Ruhr-Universität Bochum, D-44870, Germany*

²*Institute of Nuclear and Particle Physics and Department of Physics and Astronomy, Ohio University, Athens, OH 45701, USA*

We calculate the magnetic form factor of the deuteron up to $O(eP^4)$ in the chiral EFT expansion of the electromagnetic current operator. The two LECs which enter the two-body part of the isoscalar NN three-current operator are fit to experimental data, and the resulting values are of natural size. The $O(eP^4)$ description of G_M agrees with data for momentum transfers $Q^2 < 0.35 \text{ GeV}^2$.

PACS numbers: 13.75.Gx 12.39.Fe 13.40.Ks

Keywords: Effective field theory chiral perturbation theory meson exchange currents deuteron form factors

Introduction: In the past two decades chiral effective field theory (χ EFT) was fruitfully applied to few-nucleon dynamics (see Refs. [1, 2] for recent reviews). Two-nucleon potentials at next-to-next-to-next-to-leading order (N^3 LO) in the chiral expansion were developed [3, 4] which accurately describe low-energy scattering data and the static properties of the deuteron. Higher-order corrections to the three-nucleon force are presently under investigation, see e.g. [10], although discussions regarding non-perturbative renormalization of the Schrödinger equation and implications for the χ EFT power counting continue, see [5–9] for samples of different views. In parallel to these developments in the strong sector, much effort has been devoted to pionic and electroweak reactions in few-nucleon systems, see [11–13] for recent examples.

Electromagnetic reactions on light nuclei such as elastic electron scattering, photo-/electrodisintegration and radiative capture have been extensively studied in nuclear physics. In the single-photon approximation, their theoretical description requires knowledge of the electromagnetic current operator, which should be constructed consistently with the nuclear Hamiltonian. The derivation of exchange currents in χ EFT was first addressed in the seminal paper by Park et al., [14], who, however, limited themselves to threshold kinematics $|\mathbf{q}| \ll M_\pi$ with M_π denoting the pion mass. Recently, this work was extended to the general kinematics suitable to study, e.g., electron scattering off light nuclei at momentum transfer of $|\mathbf{q}|$ of order M_π by the JLab-Pisa [15–17] and Bochum-Bonn groups [18, 19]. Here and in what follows, we discuss the expansion of the irreducible two-nucleon operators J_0 and \mathbf{J} in powers of $P \equiv (p, m_\pi)/\Lambda$ with Λ denoting the hard scale in the theory, e.g. the cutoff ($\sim 600 \text{ MeV}$) used in calculations. In this expansion the leading-loop order is eP^4 . However, most of the corrections to the two-body pieces of the two-nucleon current and charge operators at this order are of isovector type and thus do not

contribute to the deuteron form factors. In particular, up to this order, the only two-body contributions to the isoscalar charge density operator, $J_0^{(s)}$ emerge from the leading relativistic corrections of one-pion range so that $J_0^{(s)}$ is parameter free. The impact of these corrections on the deuteron charge and quadrupole form factors, G_C and G_Q is studied in Refs. [20, 21]. In these works the deuteron wave functions obtained from χ EFT potentials at various orders were used to compute G_C and G_Q (see also Refs. [22, 23] for earlier work along the same lines). Good agreement with the compilation of elastic electron-deuteron data from Ref. [24] was then found for both form factors in the kinematic range $Q^2 < 0.35 \text{ GeV}^2$, provided factorization was employed in order to account for single-nucleon structure.

On the other hand, the isoscalar two-nucleon current operator, $\mathbf{J}^{(s)}$ has two two-body contributions at order eP^4 : one from a short-distance operator and one of one-pion range. The impact of these terms on the magnetic moments of the deuteron and trinucleons was examined in Ref. [25]. However, markedly more information on the interplay of these terms with each other and with one-body mechanisms is available via the $|\mathbf{q}|^2$ -dependence of observables. In this work we present a study in this direction, using χ EFT expressions for $\mathbf{J}^{(s)}$ derived in Refs. [18, 19] to extend the predictions given for G_M in Refs. [21, 23] to $O(eP^4)$. We discuss the relevant terms in the current operator and use the data on the magnetic form factor of the deuteron at low values of $|\mathbf{q}|^2$ to determine two unknown low-energy constants (LECs). The $O(eP^4)$ χ EFT results thereby obtained accurately describe experimental data on G_M in the kinematic range $Q^2 < 0.35 \text{ GeV}^2$. This, together with the findings of Ref. [21], provides a full set of results for elastic electron-deuteron form factors at $O(eP^4)$.

In the next section we describe the anatomy of the calculation and outline the relevant terms in the two-nucleon current operator. This is followed by a discussion of our results, including those for the LECs. We finish by summarizing.

Anatomy of the calculation: The magnetic form factor of the deuteron we are focused in this work is related to

*Electronic address: s.koelling@fz-juelich.de

†Electronic address: evgeny.epelbaum@rub.de

‡Electronic address: phillips@phy.ohiou.edu

the Breit-frame matrix element of the four-current operator J_μ according to the well-known relation

$$G_M = \frac{1}{\sqrt{2\eta}|e|} \langle 1|J^+|0\rangle, \quad (1)$$

where $J^+ = J^1 + iJ^2$ and $\eta = |\mathbf{q}|^2/(4m_d^2)$ with $\mathbf{q} \equiv \mathbf{p}'_e - \mathbf{p}_e$ denoting the momentum transfer and m_d the deuteron mass. (Since we work in the Breit frame we have $Q^2 = |\mathbf{q}|^2$.) The deuteron states are labelled by the projection of its spin along the direction of \mathbf{q} . Both the deuteron wave functions and the current operator appearing on the right-hand side of the above equation are calculated order-by-order in χ EFT.

We now briefly describe the χ EFT expansion of the two-nucleon current operator, J_μ , as it pertains to the calculation of the deuteron form factors. We employ Weinberg's power counting throughout this work which makes use of naive dimensional analysis to determine the significance of various contributions. The leading contribution to the charge density, J_0 , is given by an A^0 photon coupling to a point proton at order e . Nucleon-structure corrections start contributing to the one-body current at order eP^2 [next-to-leading order (NLO)]. The first isoscalar two-body contribution is generated from a tree-level pion-exchange diagram at order eP^4 , provided the nucleon mass is counted as $m_N \sim \Lambda^2/M_\pi \gg \Lambda$ [18, 19] [41]. This correction is associated with a relativistic correction to the one-pion-exchange part of the NN potential. There are numerous other corrections to the two-body part of the charge operator at leading-loop order, eP^4 , from one- and two-pion exchange diagrams and from pion loops involving the lowest-order contact interactions, but this is the only isoscalar effect. The explicit form of all terms can be found in Refs. [18, 19].

The chiral expansion of the three-current starts at order eP with the single-nucleon contributions. The first two-body terms emerge from tree-level one-pion exchange diagrams at order eP^2 [NLO]. The next two-body corrections to \mathbf{J} occur at order eP^4 from pion loops and tree diagrams involving higher-order vertices from the effective Lagrangian. The two-pion exchange contributions are parameter-free [18], while the one-pion exchange terms depend on the LECs \bar{d}_8 , \bar{d}_9 , \bar{d}_{18} , \bar{d}_{21} and \bar{d}_{22} entering $\mathcal{L}_{\pi N}^{(3)}$ [14, 26–28]. However, the only long-range two-body mechanism in $\mathbf{J}^{(s)}$ at this order is proportional to \bar{d}_9 . While this LEC could, in principle, be constrained by pion photoproduction data, in practice these data provide little information on \bar{d}_9 [29, 30].

G_M is of particular interest at $O(eP^4)$ because it is there that the first short-distance NN physics not determined by NN scattering and gauge invariance appears. This is represented by the simplest M1 isoscalar four-nucleon-one-photon contact term in the χ EFT Lagrangian, which is of the form [19, 23, 31]:

$$\mathcal{L}_{M1} = \frac{eL_2}{2} (N^\dagger \epsilon_{ijk} \sigma_i F_{jk} N) (N^\dagger N). \quad (2)$$

The low-energy constant (LEC) L_2 that appears in Eq. (2) must be extracted from data on electromagnetic reactions in the two-nucleon system.

The combination of these two effects yields a two-body isoscalar current operator $\mathbf{J}^{(s)}$ [18, 19]:

$$\begin{aligned} \mathbf{J}_{2B}^{(s)} &= 2e \frac{g_A}{F_\pi^2} d_9 \boldsymbol{\tau}_1 \cdot \boldsymbol{\tau}_2 \frac{\boldsymbol{\sigma}_2 \cdot \mathbf{q}_2}{q_2^2 + M_\pi^2} [\mathbf{q}_1 \times \mathbf{q}] \\ &+ ieL_2 (\boldsymbol{\sigma}_1 + \boldsymbol{\sigma}_2) \times \mathbf{q}_1 + (\mathbf{1} \leftrightarrow \mathbf{2}), \end{aligned} \quad (3)$$

where \mathbf{q} labels the photon momentum and $\mathbf{q}_{1/2}$ labels the momentum transfer on nucleon one/two respectively. Since G_M is determined completely by the one-body part of $\mathbf{J}^{(s)}$ up to $O(eP^3)$ the total form factor is thus

$$G_M = \frac{1}{\sqrt{2\eta}|e|} \langle 1|\mathbf{J}_{1B}^{(s)+} + \mathbf{J}_{2B}^{(s)+}|0\rangle. \quad (4)$$

Here we use factorization to compute \mathbf{J}_{1B} , i.e. we write:

$$\mathbf{J}_{1B}^{(s)+} = \frac{|e|}{M} [G_E^{(s)}(Q^2)2\mathbf{p}^+ + iG_M^{(s)}(Q^2)(\boldsymbol{\sigma}_1 \times \mathbf{q})^+], \quad (5)$$

with \mathbf{p} the momentum of the struck nucleon, and $G_E^{(s)}$ and $G_M^{(s)}$ the isoscalar single-nucleon form factors, for which we take the parameterization of Ref. [32]. The use of this ansatz for the one-body part of $\mathbf{J}^{(s)+}$ is equivalent (up to corrections that begin only two orders beyond the order to which we work) to making a χ EFT expansion for the ‘‘body’’ form factors D_M and D_E [33]. This allows us to focus on the momentum transfer at which the χ EFT expansion for the NN current operator \mathbf{J} breaks down, without having to worry whether the theory is doing a good job of describing isoscalar nucleon structure.

Results: We now evaluate the matrix elements in Eq. (4) with a variety of χ EFT deuteron wave functions computed with the NLO and NNLO χ EFT potentials and different values of the cutoffs Λ in the Lippmann-Schwinger equation and $\bar{\Lambda}$ in the spectral function. The result found for G_M with LO χ EFT wave functions and the leading piece of $\mathbf{J}^{(s)}$, denoted here as $O(eP)$, was computed in Ref. [34]. Corrections to this come both from higher-order pieces of the NN potential, V , which affect the wave function, and from the corrections to $\mathbf{J}^{(s)}$ discussed in the previous section. The NNLO χ EFT potential includes all effects up to $O(P^3)$ relative to leading (in this counting), so its deuteron wave function, when combined with the $O(eP^4)$ $\mathbf{J}^{(s)}$, yields a χ EFT calculation for G_M which includes all effects up to $O(eP^4)$.

The pertinent matrix elements are computed via Monte-Carlo (MC) integration. To increase efficiency, we use importance sampling with the weight function of Ref. [35]:

$$p(\mathbf{k}) \equiv p(k) = \frac{(r-3)(r-2)(r-1)}{8\pi} \frac{C^{r-3}}{(k+C)^r}. \quad (6)$$

The functional form of $p(k)$ is chosen such that the weight function is maximal at the origin, reflecting the large

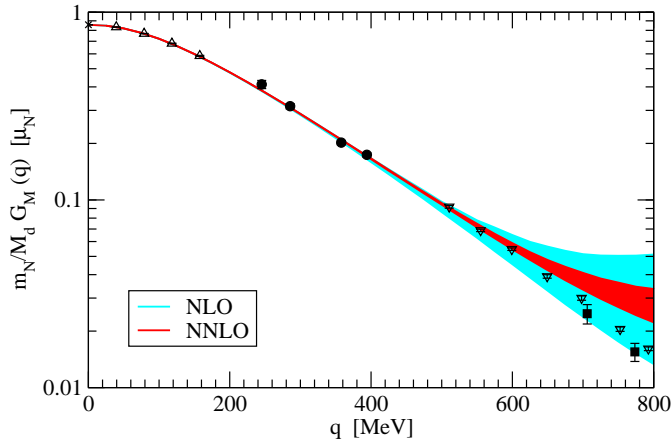


FIG. 1: (Color online) The magnetic formfactor G_M as a function of $|\mathbf{q}|$. Experimental data for the magnetic moment is from [36]. The remaining data are from the parameterization of [37] (upward triangles) and scattering experiments reported in [38] (downward triangles), [39] (squares) and [40] (solid dots). The light (dark) band represents the results with NLO (NNLO) wave functions, and $\mathbf{J}^{(s)}$ computed up to $O(eP^4)$.

S -wave component of the deuteron wave function. The parameters C and r control the vanishing of the weight function at large momenta and are tuned to optimal values (in terms of the efficiency of the MC integration) by calculating the expectation value of the one-pion exchange potential yielding $C = 1$ GeV and $r = 11$.

As in Ref. [35] we perform a path average over several runs. We use 2730 sample points and the path average is performed for 3000 runs. Analysis of the run-to-run fluctuations indicates a final answer with better than 1% precision throughout the momentum range of 0 – 800 MeV. At several points we compared this MC answer to calculations using quadrature methods, and always found agreement within the precision claimed.

We adopt the following procedure to determine the values of the two LECs entering $\mathbf{J}^{(s)}$. First, we fix the value of L_2 for a given \bar{d}_9 by demanding that the magnetic moment of the deuteron is reproduced. We then perform a χ^2 -fit to the experimental data for $|\mathbf{q}| < 400$ MeV (including four points from the parametrization of Ref. [37]) to determine \bar{d}_9 . Our attempts to use even lower- $|\mathbf{q}|$ data for this fit resulted in unstable answers, reflecting the insensitivity of G_M to this LEC at small values of $|\mathbf{q}|$.

The results of this procedure are shown in Fig. 1. The light/blue (dark/red) band is obtained using wave functions computed with the NLO (NNLO) χ EFT potential. The width of the band shows the variation of the prediction as Λ and $\bar{\Lambda}$ are changed in the range $\Lambda = 400 \dots 550$ MeV ($\bar{\Lambda} = 450 \dots 600$ MeV) at NLO (NNLO) and $\bar{\Lambda} = 500 \dots 700$ MeV. The cutoff variation is reduced at NNLO, and the data well described for $Q^2 < 0.35$ GeV².

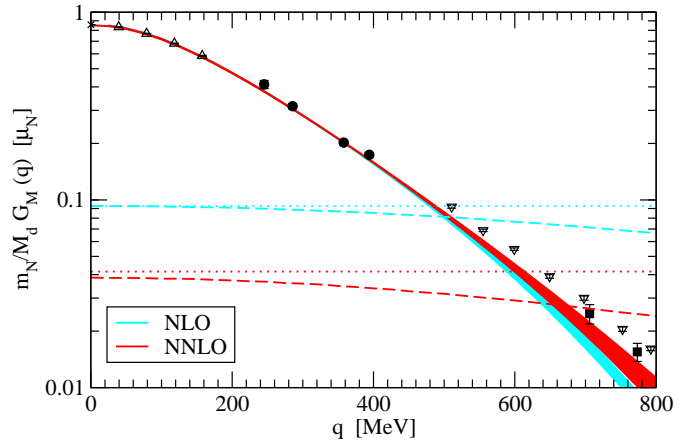


FIG. 2: (Color online) The magnetic formfactor G_M as a function of $|\mathbf{q}|$. The light (dark) band represents the results with NLO (NNLO) wave functions using the impulse approximation. The dashed/dotted lines are the contributions from two-body pieces of $\mathbf{J}^{(s)}$ (light: NLO, dark: NNLO), as described in the text. For remaining notation see Fig. 1.

In order to assess the momentum transfer at which the χ EFT expansion for $\mathbf{J}^{(s)}$ breaks down, in Fig. 2 we show the size of different contributions to the final result. This time the bands represent the impulse approximation result obtained with NLO (light/blue) and NNLO (dark/red) wave functions. The dotted (dashed) line is the effect from the piece of $\mathbf{J}_{2B}^{(s)}$ that is proportional to L_2 (\bar{d}_9). For both two-body matrix elements, we show results averaged over the five cutoff combinations considered, with the light blue lines showing the NLO case, and the dark red lines obtained with NNLO wave functions. We estimate the breakdown scale of the EFT expansion by values of momentum transfer at which the $O(eP^4)$ two-body contributions start becoming comparable to the effect of the $O(eP)$ (impulse-approximation) piece of the current. Fig. 2 shows that the smaller two-body contributions to G_M found with the NNLO wave function delay the breakdown of the expansion. Even so, we would infer a breakdown scale $|\mathbf{q}| = 600$ MeV, as there the short-distance effect $\sim L_2$ becomes equal in magnitude to the impulse-approximation result.

In Table I we present the values of \bar{d}_9 and L_2 obtained in our fits. Small values of \bar{d}_9 are preferred, which is consistent with the findings of Ref. [29]. Reassuringly, the inferred values of \bar{d}_9 show only a very mild dependence on the cutoffs as compared to the expected natural size of this LEC, $|\bar{d}_9| \sim 1$ GeV⁻². In contrast, the values of L_2 do depend on the choice of the regulator employed for the NN potential, as one would expect. It is comforting to see that all obtained values of L_2 are natural with respect to the cutoff scale Λ employed in these calculations. The values of L_2 reported in the table show that two-body effects in G_M play a larger role in the calculation with

NLO deuteron wave functions, as seen in Fig. 2.

Summary: The first two-body effects in the deuteron magnetic form factor G_M , occur at $O(eP^4)$ in χ EFT, i.e. three orders beyond leading. Inclusion of these mechanisms in the computation of G_M improves the description of data, and allows exact reproduction of the deuteron magnetic moment, which otherwise is underpredicted in χ EFT. Experimental data is then well described for $Q^2 < 0.35 \text{ GeV}^2$, and the chiral expansion for G_M is found to converge well for $Q^2 < 0.25 \text{ GeV}^2$, provided that the NNLO wave functions of Ref. [4] are employed. Finally, we note that the proposal of Ref. [6] to change the scaling of short-distance χ EFT operators in order to ensure proper renormalization of the theory does not significantly alter the relative importance of such operators in the ${}^3\text{S}_1$ - ${}^3\text{D}_1$ channel [8]. Therefore we expect that the conclusions of this study will be quite robust with respect to developments on this front.

Acknowledgements

We thank Ulf-G. Meißner for useful comments on the manuscript. This work is supported by the EU Hadron-

Physics3 project “Study of strongly interacting matter”, by the European Research Council (ERC-2010-StG 259218 NuclearEFT), by the DFG (TR 16, “Subnuclear Structure of Matter”), and by the US Department of Energy (contract no. DE-FG02-93ER40756).

Order	$\Lambda/\bar{\Lambda}$ [MeV]	\bar{d}_0 [GeV^{-2}]	L_2 [GeV^{-4}]
NLO	400/500	-0.010	0.243
NLO	400/700	-0.011	0.249
NLO	550/500	0.016	0.605
NLO	550/600	0.017	0.731
NLO	550/700	0.018	0.892
NNLO	450/500	-0.011	0.188
NNLO	450/700	-0.009	0.173
NNLO	550/600	0.005	0.089
NNLO	600/500	0.001	0.113
NNLO	600/700	-0.001	0.028

TABLE I: Values for \bar{d}_0 and L_2 found by fitting data up to $|\mathbf{q}| = 400 \text{ MeV}$, using different values of the cutoffs.

-
- [1] E. Epelbaum, H.-W. Hammer and U.-G. Meißner, *Rev. Mod. Phys.* **81**, 1773 (2009).
- [2] E. Epelbaum and U.-G. Meißner, arXiv:1201.2136 [nucl-th].
- [3] D. R. Entem and R. Machleidt, *Phys. Rev. C* **68**, 041001 (2003).
- [4] E. Epelbaum, W. Glöckle and U.-G. Meißner, *Nucl. Phys. A* **747**, 362 (2005).
- [5] G. P. Lepage, nucl-th/9706029.
- [6] A. Nogga, R. G. E. Timmermans and U. van Kolck, *Phys. Rev. C* **72**, 054006 (2005).
- [7] E. Epelbaum and U.-G. Meißner, nucl-th/0609037.
- [8] M. C. Birse, *Phys. Rev. C* **74**, 014003 (2006).
- [9] M. Pavon Valderrama and E. Ruiz Arriola, *Phys. Rev. C* **74**, 054001 (2006).
- [10] H. Krebs, A. Gasparyan and E. Epelbaum, *Phys. Rev. C* **85**, 054006 (2012).
- [11] V. Baru, C. Hanhart, M. Hoferichter, B. Kubis, A. Nogga and D. R. Phillips, *Phys. Lett. B* **694**, 473 (2011).
- [12] D. Gazit, S. Quaglioni and P. Navratil, *Phys. Rev. Lett.* **103**, 102502 (2009).
- [13] H. W. Griesshammer, J. A. McGovern, D. R. Phillips and G. Feldman, arXiv:1203.6834 [nucl-th].
- [14] T. -S. Park, D. -P. Min and M. Rho, *Nucl. Phys. A* **596**, 515 (1996).
- [15] S. Pastore, R. Schiavilla and J. L. Goity, *Phys. Rev. C* **78**, 064002 (2008).
- [16] S. Pastore, L. Girlanda, R. Schiavilla, M. Viviani and R. B. Wiringa, *Phys. Rev. C* **80**, 034004 (2009).
- [17] S. Pastore, L. Girlanda, R. Schiavilla and M. Viviani, *Phys. Rev. C* **84**, 024001 (2011).
- [18] S. Kölling, E. Epelbaum, H. Krebs and U.-G. Meißner, *Phys. Rev. C* **80**, 045502 (2009).
- [19] S. Kölling, E. Epelbaum, H. Krebs and U.-G. Meißner, *Phys. Rev. C* **84**, 054008 (2011).
- [20] D. R. Phillips, *Phys. Lett. B* **567**, 12 (2003).
- [21] D. R. Phillips, *J. Phys. G* **34**, 365 (2007).
- [22] D. R. Phillips and T. D. Cohen, *Nucl. Phys. A* **668**, 45 (2000).
- [23] M. Walzl and U.-G. Meißner, *Phys. Lett. B* **513**, 37 (2001).
- [24] D. Abbott *et al.* [JLAB t20 Collaboration], *Eur. Phys. J. A* **7**, 421 (2000).
- [25] Y. -H. Song, R. Lazauskas, T. -S. Park and D. -P. Min, *Phys. Lett. B* **656**, 174 (2007).
- [26] G. Ecker and M. Mojžiš, *Phys. Lett. B* **365**, 312 (1996).
- [27] N. Fettes, U.-G. Meißner and S. Steininger, *Nucl. Phys. A* **640**, 199 (1998).
- [28] J. Gasser, M. A. Ivanov, E. Lipartia, M. Mojžiš and A. Rusetsky, *Eur. Phys. J. C* **26**, 13 (2002).
- [29] A. Gasparyan and M. F. M. Lutz, *Nucl. Phys. A* **848**, 126 (2010).
- [30] H. W. Fearing, T. R. Hemmert, R. Lewis and C. Unkmeir, *Nucl. Phys. A* **684**, 377 (2001).
- [31] J. W. Chen, G. Rupak and M. J. Savage, *Nucl. Phys. A* **653**, 386 (1999).
- [32] M. A. Belushkin, H. W. Hammer and U.-G. Meißner, *Phys. Rev. C* **75**, 035202 (2007).
- [33] R. A. Gilman and F. Gross, *J. Phys. G* **28**, R37 (2002).
- [34] M. Pavon Valderrama, A. Nogga, E. Ruiz Arriola and D. R. Phillips, *Eur. Phys. J. A* **36**, 315 (2008).
- [35] S. Liebig, V. Baru, F. Ballout, C. Hanhart, A. Nogga [arXiv:1003.3826/nucl-th]
- [36] I. Lindgren, in: K. Siegbahn (ed.), in: *Alpha-, Beta- and Gamma-Ray Spectroscopy*, Vol. 2, North-Holland, Amsterdam 1965.

- [37] I. Sick, Prog. Part. Nucl. Phys. **47**,(2001) 245.
- [38] S.Auffret et. al, Phys. Rev. Lett **54**,(1985) 649.
- [39] R.Cramer et. al, Z. Phys. C **29**,(1985) 513.
- [40] G. G. Simon, C. Schmidt, V. H. Walther, Nucl. Phys. A **364**,(1981) 285.
- [41] In the nomenclature of Refs. [18, 19], these contributions appear at $O(eQ)$.